IOP PUBLISHING JOURNAL OF PHYSICS D: APPLIED PHYSICS

J. Phys. D: Appl. Phys. **40** (2007) 7675–7681 doi:10.1088/0022-3727/40/24/013

Current–voltage (I–V) studies of Mo/γ-In_2Se_3/ZnO : Al diode structures

M Morsli[1], C Amory, A Bougrine, L Cattin and J C Bernède

Université de Nantes, Nantes Atlantique Universités, LAMP, EA 3825, Faculté des Sciences et des Techniques, 2 rue de la Houssinière, BP 92208, Nantes, F-44000 France

E-mail: Mustapha.morsli@univ-nantes.fr

Received 1 August 2007, in final form 14 September 2007
Published 30 November 2007
Online at stacks.iop.org/JPhysD/40/7675

Abstract

Mo/γ-In_2Se_3/ZnO : Al diode structures have been grown by vacuum deposition. In order to study the influence of the ZnO : Al electrode on the diode properties, ZnO : Al conductive and insulating films have been deposited by rf magnetron sputtering using a single Al_2O_3 doped ZnO target. These films have been characterized before their use in diodes. The electrical properties of ZnO : Al are controlled by the oxygen partial pressure during deposition. The effect of the composition on the I–V characteristics of γ-In_2Se_3 based diodes has been investigated. When γ-In_2Se_3 is doped with manganese there is no photovoltaic effect while there is when it is pure. It is shown that the I–V curves agree with Schottky theory only in the case of pure γ-In_2Se_3. When it is doped the I–V curves agree well with the trap-controlled space charge limited transport theory, which is attributed to the presence of a band of localized states present in the band gap of γ-In_2Se_3 after Mn doping.

1. Introduction

In recent years indium selenide semiconductors have been a subject of interest in thin films form because of their properties that make them attractive for device applications [1–4]. In_2Se_3 is one of the most extensively studied binary III–VI chalcogenides. There are many phases of this compound and γ-In_2Se_3 appears as the stable phase at room temperature [5,6]. In earlier papers, we have shown that In_2Se_3 films can be easily obtained by co-evaporation. With this technique, the films are homogeneous and uniform, textured and free of any other phase than the γ phase. However, if these films are single phased with good crystalline quality, they are too resistive for competitive solar cells applications [7]. More recently, we have shown that highly conductive and photoconductive films can be obtained by Mn doping [8]. For optimum Mn doping the room temperature conductivity is six orders of magnitude higher than that of pure γ-In_2Se_3 films.

In this work, doped and pure γ-In_2Se_3 films have been used in diode structures glass/Mo/γ-In_2Se_3/ZnO : Al. By analogy with Cu(In,Ga)Se_2 (CIGS) based solar cells, the bottom electrode used was a Mo film [9] and the upper electrode was a ZnO : Al film. It has been shown that better performances can be obtained when a thin oxide film of low conductivity is introduced between the CIGS film and the conductive ZnO : Al [10]. We have probed the influence of such an oxide bilayer on the performances of the γ-In_2Se_3 based diodes. To grow such a bilayer, usually, two ZnO targets are used: one is pure ZnO and the other is Al_2O_3 doped ZnO [10].

In this work we have used only one doped target (ZnO with 2 wt% of Al_2O_3), the oxide conductivity being monitored by the oxygen partial pressure during deposition.

Therefore, after the description of the properties of such a bilayer ZnO : Al upper electrode, we report the results of the current–voltage studies of diode structures to get information about their conductivity processes and band gap.

2. Experimental

γ-In_2Se_3 films have been deposited by thermal co-evaporation as described in [7]. When γ-In_2Se_3 : Mn films were used, the film elaboration process is divided into two stages. In the first, a thin layer of Mn is deposited, then we proceed to the co-evaporation. The films were elaborated in a vacuum chamber from elemental sources with resistively heated tungsten (In, Mn) and molybdenum (Se) crucible

[1] Author to whom any correspondence should be addressed.

sources. An HF quartz oscillator is used to control the evaporation rate of Mn (0.3 nm s^{-1}), Se (15 nm s^{-1}) and to calibrate that of In (0.12 nm s^{-1}) according to the temperature of the crucible. The substrates used are soda lime glass and Mo coated soda lime glass. They are heated by an infra red source. The temperature of the substrate is determined by a thermocouple (type K) on the deposition face and is kept constant at 300 °C, since it has been shown earlier that this temperature is optimum to grow textured γ-In_2Se_3 thin films. The Se vapour pressure is very high, and therefore during deposition onto a substrate at 300 °C [7, 8], the excess selenium re-evaporates and the growth rate of the γ-In_2Se_3 film is controlled by the In deposition rate. The residual pressure during the entire elaboration process does not exceed 3×10^{-5} bar. The thickness of the Mn layer was 4.5 nm, since we have shown earlier [8] that the best results are obtained with such a precursor thickness, when the whole thickness of the γ-In_2Se_3 : Mn film is around 1 μm, which is the thickness used in the diode structures. Under such experimental conditions we have $y = 0.008$, y being the atomic concentration ratio with y = [Mn]/([Mn] + [In] + [Se]). It should be noted that the thickness of all the In_2Se_3 films, Mn doped or non-doped, was around 1 μm.

In the case of diode structures, the bottom electrode was a Mo film deposited by sputtering. The properties of these Mo films have been reported earlier [9]. In short, Mo films have been deposited by rf sputtering, as proposed by Scofield *et al* [11], a two pressure deposition process has been used: a short (10 min) high argon pressure (6 Pa) step to grow a resistive but adhesive layer, followed by a low pressure (1.45 Pa) step to achieve low sheet resistance. Finally, the whole Mo film thickness is around 1.5 μm.

We have shown that the optimum substrate holder–target distance is 5 cm in the diode rf apparatus used [9]. The films deposited under such conditions are crystallized. The crystallites are columnar and perpendicular to the plane of the substrate. The resistivity of the Mo films is in the range 40–80 $\mu\Omega$ cm. Their adherence properties are proven by their stability after γ-In_2Se_3 : Mn deposition at 300 °C.

The upper electrode was an aluminium doped zinc oxide layer, in order to built a p–n junction between the p-type γ-In_2Se_3 and the n-type ZnO : Al.

About the upper electrode, the zinc oxide films were deposited by ac magnetron sputtering on glass substrates at room temperature. The plasma generation chamber is surrounded by an electromagnet. A cylindrical target of diameter 75 mm and thickness of 5 mm was prepared by sintering the mixture of ZnO powder (purity of 99.99%) with 2 wt% Al_2O_3 (purity 99.99%). Ar (99.99%) as well as Ar/O_2 mixture with 2% O_2 gas sources are used as sputtering gas for deposition of the ZnO : Al films. The distance between the target and the substrate was about 60 mm. The flow rates of both argon and argon/oxygen were controlled by using the flow meter. The sputtering pressure was maintained at 0.13 Pa. The pressure of the sputtering system before the deposition of the sample films was under 2×10^{-3} Pa. The films were deposited onto glass substrates under conditions listed in table 1. These deposition conditions were fixed in order to study the influence of oxygen partial pressure on ZnO : Al films' properties.

The crystalline structure of the films was analysed by x-ray diffraction (XRD) by a Siemens D 5000 diffractometer using

Table 1. Experimental RF magnetron sputtering conditions.

Parameter	Magnitude
Target–substrate distance	60 mm
Sputtering pressure	0.13 Pa
Power deposition	150 W
Flow gas	35 sccm
Sputtering time	20 min
Oxygen partial pressure	0–2%

Kα radiation from Cu ($\lambda = 0.15406$ nm). The morphology and structure cross section were observed through scanning electron microscopy (SEM) with a JEOL 6400F. A simple software program allows us to deduce the thickness of the films from the cross section visualization. The composition of the films was checked by an electron microprobe analysis (EMPA) using a JEOL 5800. Optical transmission spectra were recorded by a Carry spectrophotometer. The absorption coefficient α of the films was calculated from the transmittance of two samples of different thicknesses, grown under the same conditions, as described by Bichel and Levy [12]. In that case α is

$$\alpha = 1/(t_2 - t_1)\mathrm{Ln}(T_1/T_2)$$

with T the transmittance and t the thickness.

Any errors incurred in the values of uncertainties induced by this technique are much less than the errors in the thickness measurements, which dominate the experimental errors. The junction properties were evaluated in terms of current density–voltage (I–V) characteristics. The illuminated characteristics were measured under standard AM 1.5 illumination using a solar simulator (ORIEL, model 81150).

3. Results

All the chalcogenides films are stoichiometrics as checked by the EMPA analysis. The pure and Mn doped γ-In_2Se_3 films were crystallized in the expected wurtzite-like structure [13]. However if no crystallite texturation can be achieved in the case of the γ-In_2Se_3 : Mn films deposited onto the Mo coated glass, a strong preferential orientation can be obtained in the case of pure films (figure 1). However, if it is easy to grow textured γ-In_2Se_3 films when they are deposited onto bare glass [7], it is not so easy when a Mo film covers the glass substrate. A careful study shows that, when optimum conditions are not strictly obeyed ($T_s = 300$ °C, evaporation rate of In 0.12 nm s^{-1}, clean molybdenum surface), the pure γ-In_2Se_3 films are not textured. When optimum conditions are used the texturation coefficient F_{006} of around 80% can be achieved (figure 1(*a*)). Moreover, for the same film thickness the peak intensity is far higher in the case of the textured pure γ-In_2Se_3 films. No such results have been achieved with Mn doped γ-In_2Se_3 films. Consequently the c axis of the grains is perpendicular to the substrate in the case of pure γ-In_2Se_3 films, while it is randomly oriented in the case of γ-In_2Se_3 : Mn films. Recently, a new metastable phase of indium selenium has been put in evidence; it is called κ-In_2Se_3 [14, 15]. In a publication devoted to the study of the growth instability of γ-In_2Se_3 we have proposed the presence of this metastable phase during the growth of the film in a certain domain of substrate temperature (between 550 and 650 K), which induces randomly oriented thin films [7].

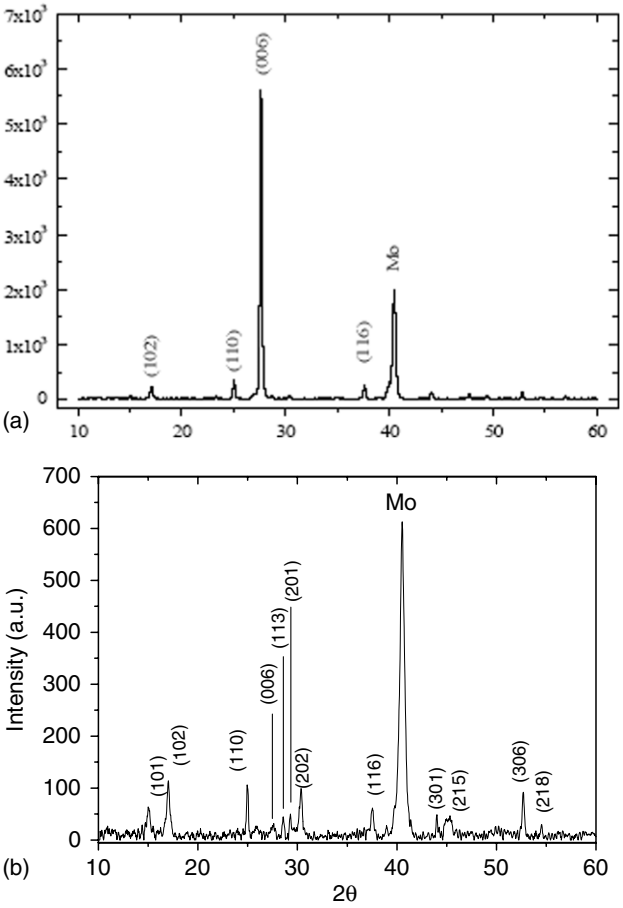

Figure 1. XRD diagram of a γ-In_2Se_3 deposited onto Mo coated glass: (a) pure film, (b) Mn doped thin film.

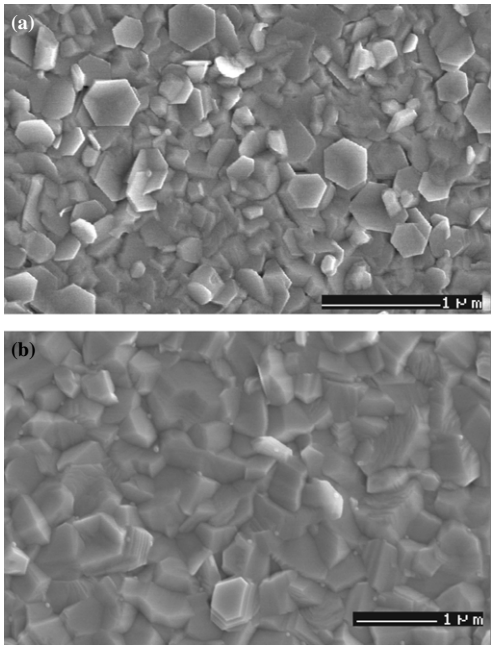

Figure 2. Microphotographs of γ-In_2Se_3 films: (a) pure film, (b) Mn doped thin film.

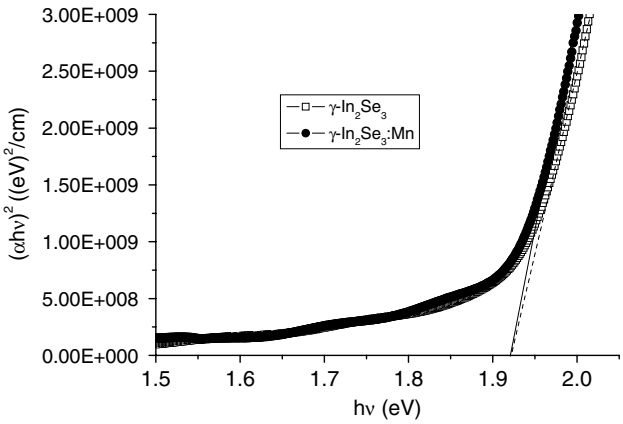

Figure 3. $(\alpha h\nu)^2$ versus hν or pure and Mn doped γ-In_2Se_3 films.

The XRD study is confirmed in figure 2. This figure shows the SEM visualization of typical γ-In_2Se_3 thin films surfaces. One can see that both families of films are homogeneous without any hole. Moreover crystallites parallel to the plan of the substrate with a hexagonal shape can be seen in the case of non-doped γ-In_2Se_3 (figure 2(a)), which is not the case of γ-In_2Se_3 : Mn (figure 2(b)). This observation is in good agreement with the XRD study.

Some films have been deposited onto the glass substrate in order to proceed to some electrical and optical measurements. At room temperature the dark conductivity of γ-In_2Se_3 is around $10^{-7}\,\mathrm{S\,cm^{-1}}$, while that of γ-In_2Se_3 : Mn is (3–5) $\times$ $10^{-2}\,\mathrm{S\,cm^{-1}}$. The carrier majority type has been checked by the hot probe technique; all the films are p-type. If we define the photoconductivity σ_{Ph} of the films as $\sigma_{Ph} = \sigma_{Illuminated} - \sigma_{Dark}$, we have $\sigma_{Ph} = 7.7 \times 10^{-5}\,\mathrm{S\,cm^{-1}}$ for γ-In_2Se_3 and $\sigma_{Ph} = 7.5 \times 10^{-1}\,\mathrm{S\,cm^{-1}}$ with γ-In_2Se_3 : Mn. Therefore it can be said that electrical properties of the films are improved after Mn doping, while their structural properties are degraded.

About the optical study, it can be seen in figure 3 that neither the shape of the curves nor the value of the band gap depend on Mn doping. The direct band gap of the films has been deduced from the extrapolation of the linear part of the graph relative to the function $(\alpha h\nu)^2 = f(h\nu)$. The estimated band gap value, E_g, is around 1.92 eV.

After these characterizations, the γ-In_2Se_3 films have been probed in diode structures. In order to test them as a possible absorber layer in solar cells, the upper electrode should be transparent in the visible and ZnO : Al films have been used.

As mentioned above the ZnO : Al films were deposited by sputtering, under the conditions of table 1. Since only one ZnO doped target has been used to grow conductive and no-conductive ZnO : Al films, we have systematically studied the properties of the films and their variations with the partial pressure of oxygen during sputtering.

Zinc oxide crystallizes in the hexagonal system with a wurtzite structure. Figure 4 displays XRD patterns of ZnO : Al films under pure Ar and Ar with a 2% of O_2. These results show that all the deposited films are polycrystalline, crystallized in the hexagonal wurtzite structure with the crystallites preferentially oriented along the c axis (0 0 2) perpendicular to the substrate surface. As shown in figure 4, by changing the O_2/Ar ratio, the location of the observed diffraction peaks remained almost identical.

We have also examined the influence of the sputtering atmosphere on the full width at half maximum (FWHM) of the

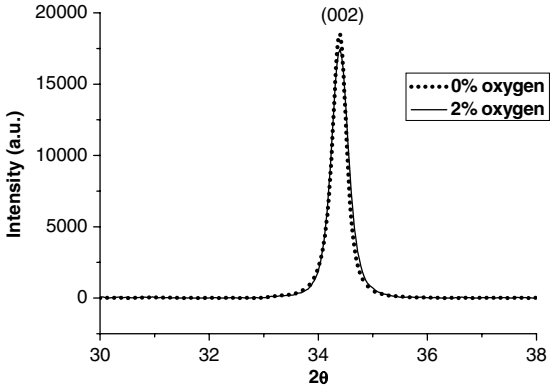

Figure 4. XRD diagram of ZnO:Al films sputtered in pure Ar atmosphere (. . .) and in pure Ar + 2%O_2 atmosphere (——).

Table 2. X-ray diffraction characterization.

	Oxygen in at%	
Parameter	0	2
c (Å)	5.2194	5.2064
FWHM	0.328 ± 0.020	0.333 ± 0.020

Table 3. Microprobe analysis.

Elemental composition (at% ±1.0)	Oxygen partial pressure (%)	
	0%	2%
Zn	50.0	49.2
O	48.0	49.0
Al	2.0	1.8

x-ray diffraction peak of (0 0 2) and on the lattice parameter, which can be calculated using the formula

$$d_{hkl} = \frac{1}{\sqrt{4(h^2 + k^2 + l^2)/(3a^2) + (l^2/c^2)}}$$

The obtained results are presented in table 2. They are not significantly different from the reference values [16]. Also the FWHM value of the (0 0 2) peak is not clearly related to the oxygen partial pressure. It should be noted that the values reported are mean values calculated from, at least, five samples.

The measurements of the films' composition have been done by EPMA analysis. This technique allows estimation of the oxygen atomic concentration; however the precision of the measure decreases with the atomic weight of the element; therefore, as shown in table 3, no significant evolution with oxygen partial pressure is evident in the precision range of the apparatus. However, a tendency of an increase in the oxygen content when O% increases during sputtering is probable.

Figure 5 exhibits the transmission spectra of ZnO : Al films prepared under pure Ar and Ar with 2% of O_2. Average transmissions of above 90%, in the visible range, are systematically obtained. These spectra clearly show the existence of interference fringes for all samples, which show their homogeneity. This figure also shows the presence of an important reflection in the IR region in samples deposited using pure argon gas. This should be attributed to high absorption due to the free-carriers in this region.

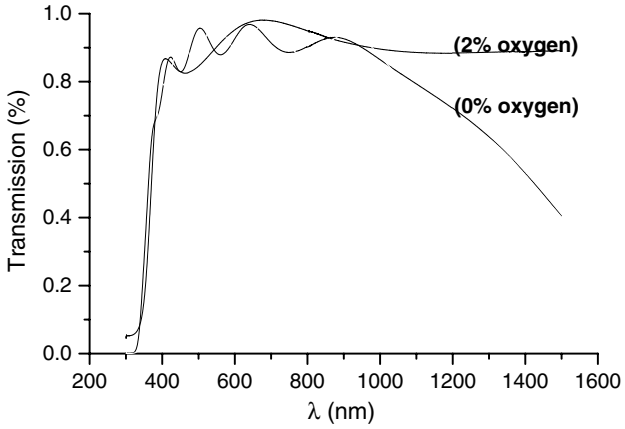

Figure 5. Transmission spectra of ZnO : Al films sputtered in pure Ar and Ar + 2%O_2 atmosphere.

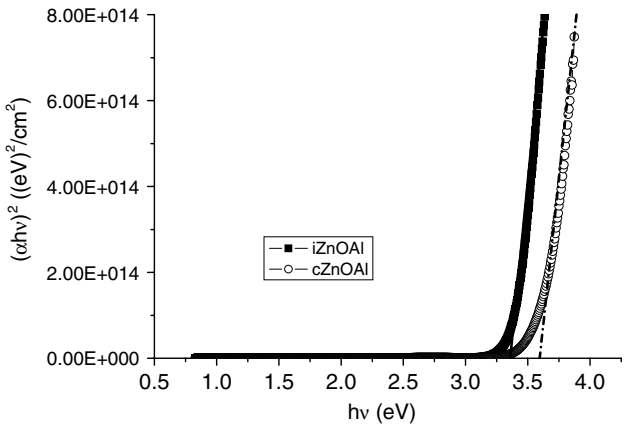

Figure 6. $(\alpha h\nu)^2$ versus hν or ZnO : Al films sputtered in pure and Ar + 2%O_2 atmosphere.

It should be noted here that, as testified by their closer fringes, the films deposited under pure argon were thicker than those deposited under Ar with 2% of O_2, and their optical properties cannot be directly compared. However, the transmission curves show the small absorbance of all the ZnO : Al films, which is the required properties for these films used as transparent electrodes in solar cells. Their difference in thickness is related to the fact that, in the devices, the films deposited under pure argon are thick (1 μm), because as seen below they are used as a conductive electrode, while those deposited under Ar with 2% of O_2 are thin (0.2 μm) because they are used as a no conducting buffer layer .

ZnO being a direct band gap semiconductor, from the plot of $(\alpha h\nu)^2$ as a function of the photon energy $(h\nu)$, the band gap values were obtained by the extrapolation of the curves for two typical samples and were found to be 3.35 and 3.6 eV for samples deposited in the presence of 2% of oxygen and without oxygen, respectively, (figure 6).

In table 4 we have given, at room temperature, the electrical conductivity, carrier concentration and Hall mobility of ZnO : Al thin films prepared at different deposition conditions. The data indicate that, as expected, the conductivity of the samples decreases when the oxygen partial pressure increases since electrical conductivity (σ) in semiconductors depends on the carrier concentration (n).

Table 4. Electrical properties of typical ZnO films.

Sample	Oxygen partial pressure (%)	Electrical conductivity σ (Ω^{-1} cm^{-1})	Carrier density n (cm^{-3})	Carrier mobility μ (cm^2 V^{-1} s^{-1})
A	0	2.32×10^3	1.16×10^{21}	12.5
B	2	3.35×10^{-1}	1.00×10^{18}	2

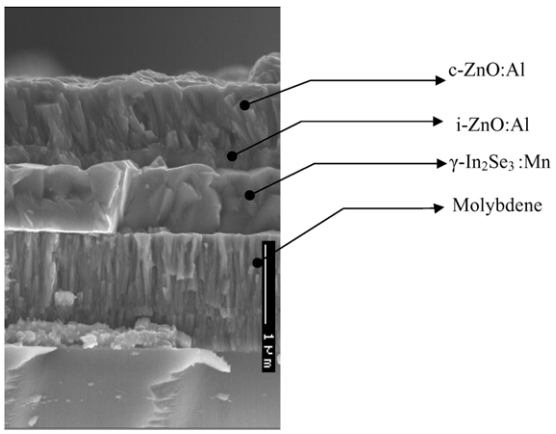

Figure 7. Cross section visualization of a glass/Mo/γ-In_2Se_3 : Mn/i-ZnO : Al/c-ZnO : Al diode structure.

Therefore, high conductivity films need high carrier concentration. Carriers in ZnO films can be provided by oxygen vacancies and/or cation substitution (Zn by Al), which justifies the higher conductivity of films deposited under a pure argon atmosphere. In n-type semiconductors heavily doped, such as transparent conductive oxide, the Fermi level is inside the conduction band by a quantity of ΔE_g. Since the states below the Fermi level are filled, fundamental transitions to states below $E_g + \Delta E_g$ are forbidden. Hence this shift of the absorption edge due to band filling is called the Burstein–Moss shift [17] and it is $\Delta E_g = E'_g - E_g = h^2/8m^*(3N/\pi)^{2/3}$, with h the Planck constant, m^* the effective mass of the electrons and N the majority carrier density. This Burstein–Moss shift justifies the fact that the band gap of films deposited in pure Ar atmosphere is broader than that of films deposited in pure Ar + 2% of O_2.

Therefore our ability to grow highly conductive (c-ZnO : Al) and poorly conductive (i-ZnO : Al) films allows us to probe γ-In_2Se_3 : Mn based diodes with, as an upper electrode, either a monolayer c-ZnO : Al or a bilayer i-ZnO/c-ZnO.

After optimization of the properties of the ZnO films, different diode configurations have been probed: Mo/γ-In_2Se_3 : Mn/c-ZnO : Al, Mo/γ-In_2Se_3/c-ZnO : Al, Mo/γ-In_2Se_3 : Mn/i-ZnO : Al/c-ZnO : Al. A typical cross section of the last structure is visible in figure 7. The different layers are clearly visible. The c-ZnO:Al film thickness is around 1 μm and that of i-ZnO : Al is 0.2 μm. The adherence between the different layers is good; the γ-In_2Se_3 : Mn grain size is similar to the thickness of the film. Typical dark and illuminated current–voltage curves, under AM 1.5 at room temperature, are presented in figure 8(a), when the absorbing layer used is γ-In_2Se_3 : Mn. It can be seen that in the dark the cell exhibits a good rectifying effect, which nearly disappears under illumination. For more than one month, the diodes were been probed nearly daily. The phenomenon is reproducible and does not deteriorate the cell. It is observed with or without the i-ZnO buffer layer. When the absorbing layer is γ-In_2Se_3, a small photovoltaic effect is measured (figure 8(b)), here also with or without the buffer layer.

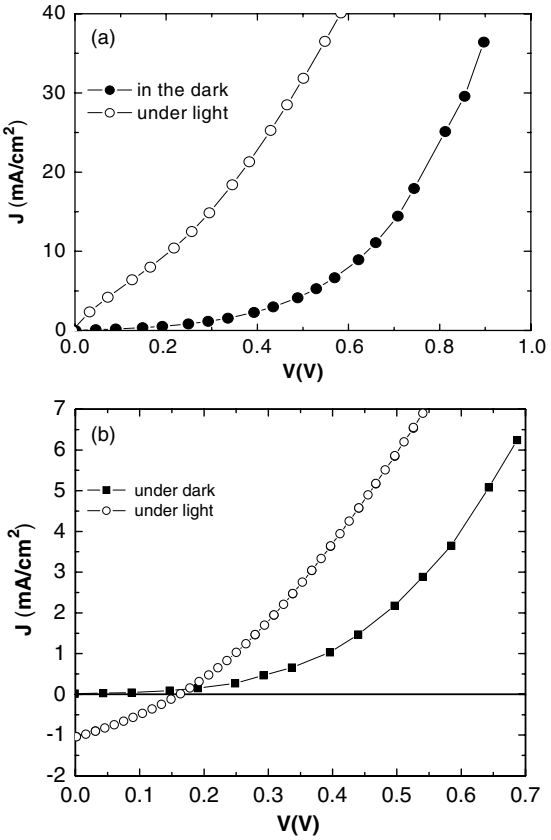

Figure 8. Dark and illuminated I–V characteristics of a glass/Mo/γ-In_2Se_3/ c-ZnO : Al: (a) Mn doped and (b) no doped γ-In_2Se_3. Inset (b): Ln $J = (V)$ for glass/Mo/γ-In_2Se_3/c-ZnO : Al.

4. Discussion

Since with or without i-ZnO : Al the results are similar whatever the γ-In_2Se_3 used, in order to discuss the most simple structure, the discussion below is devoted to Mo/γ-In_2Se_3/c-ZnO : Al. In that case, the c-ZnO : Al behaves like a degenerated semiconductor and the contact between the n$^+$c-ZnO : Al and the p-type γ-In_2Se_3 is similar to a Schottky contact.

First, we are going to discuss the γ-In_2Se_3 : Mn based diodes.

Since the structures are similar to Schottky diodes, the I–V characteristics should be described by the standard diode equation:

$$J = J_s\left[\exp - \left(\frac{qV}{nkT}\right) - 1\right], \qquad (1)$$

where q is the element charge, V the applied voltage, T the temperature (K), k the Boltzmann constant, J_s the reverse saturation current and n the diode quality factor.

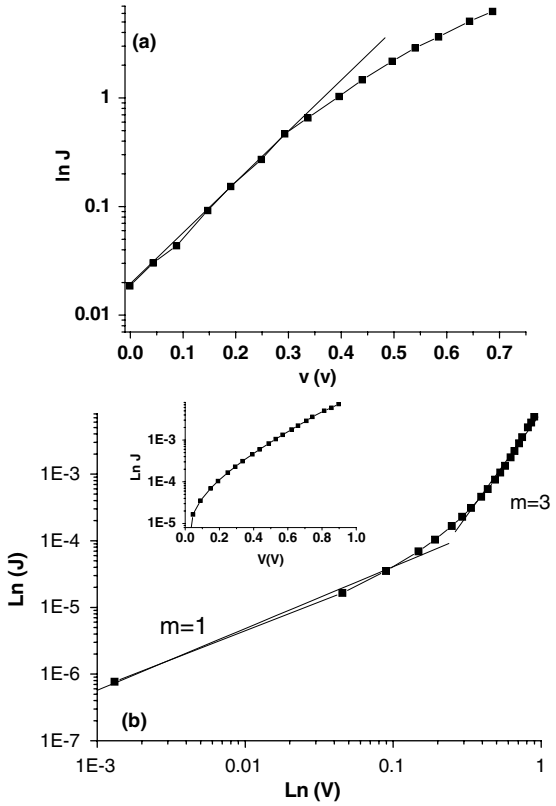

Figure 9. (*a*) Ln $J = (V)$ for glass/Mo/γ-In_2Se_3 /c-ZnO : Al. (*b*) Ln $J = f(\mathrm{Ln}(V))$ for glass/Mo/γ-In_2Se_3 : Mn/c-ZnO : Al. Insert (*b*) Ln $J = f(V)$ for glass/Mo/γ-In_2Se_3 : Mn/c-ZnO : Al.

Often, when the voltage increases, the curves deviate from the experimental behaviour indicating the effect of series resistance. A simple series resistance model can be applied in an attempt to linearize the characteristics:

$$J = J_s \left[\exp -q \left(\frac{V - JR_s}{nkT} \right) \right]. \qquad (2)$$

A simple way to check if the structures have the expected behaviour for a Schottky diode is to plot $\mathrm{Ln}(J) = f(V)$. Usually, up to an upper voltage limit the curve is linear, then the series resistance cannot be neglected and the curve bends down relatively to the theoretical straight line. It can be seen in the inset of figure 9(*b*) that, in the case of γ-In_2Se_3 : Mn based diodes, even for small voltage, the experimental curve does not correspond to the expected straight line. In fact, the Schottky barrier effect is not predominant; the conductivity process seems controlled by different less efficient effects such as bulk effect and interface traps. In order to investigate the dominant processes in the different potential regions the curve $\mathrm{Ln}(J) = f(\mathrm{Ln}(V))$ is shown in figure 9(*b*).

Between 0.001 and 0.1 V the slope of the curve is around $m = 1$, the characteristics show an 'ohmic like' region with J proportional to V. Then, for higher voltage, the slope increases and J is proportional to V^m with $m = 3$. The current is space charge limited; it is a SCLC region. Usually when there are no traps in the semiconductor or when these traps are located on a discrete levels we have $m = 2$.

However, here, m is greater than 2, which indicates the energy distribution of traps instead of discrete levels [1].

The shape of the forward characteristics under illumination is quite different. In the higher voltage domain they cannot be interpreted in terms of SCLC theory (space charge limited current). This is understandable since the carriers are generated by light in the sample nearly uniformly from one electrode to the other. The charge carrier gradient that arises when carriers are injected at the contact, which induces the field necessary for the SCLC effect, is not present when the carriers are induced by absorption of light.

In the case of γ-In_2Se_3 based diodes there is a small photovoltaic effect (figure 8(*b*)) and, as shown in figure 9(*a*), up to an upper voltage limit of about 0.35 V, the curve $\mathrm{Ln}(J) = f(V)$ is linear, which shows that these structures have the expected behaviour for a Schottky diode.

Different hypotheses can be proposed to justify such different behaviours. First of all, we have shown earlier [8] that the substitution or the insertion of manganese in the γ-In_2Se_3 thin films generates a band of localized states in its band gap. It appears from the above discussion that such localized states could prohibit the Schottky contact formation and induce the ohmic behaviour of the contact γ-In_2Se_3/c-ZnO : Al at low voltage and the SCLC effect at higher voltage. In the case of pure γ-In_2Se_3 these localized states are not present in the band gap [8] and a Schottky contact can be obtained. It is well known that the formation or not of a Schottky barrier depends strongly on the presence of interface states at the contact. As shown here, when γ-In_2Se_3 is deposited onto Mo coated glass substrates, the texturation of the film depends strongly on the deposition conditions and on the doping of the films. Pure γ-In_2Se_3, when deposited in optimum conditions, can be textured with the c axis perpendicular to the plan of the substrate, while Mn doped films cannot. Crystallites with their c axis perpendicular to the plan of the substrate have their basal (0 0 l) planes parallel to the substrate. It has been shown that with hexagonal semiconductors these planes are chemically inert, while a lot of dangling bonds can be present in the plan perpendicular to this direction [18, 19]. In the case of γ-In_2Se_3 : Mn, the crystallites are randomly oriented, which should induce a high dangling bond density at the interface and therefore prohibits Schottky contact formation. With γ-In_2Se_3 the majority of crystallite planes in contact with the upper electrode are chemically inert and a Schottky contact can be obtained. However, the conductivity of pure γ-In_2Se_3 is very small and its photoconductivity effect quite small which justify the small efficiency of these cells.

Therefore it can be concluded that when a Schottky contact is achieved at the interface γ-In_2Se_3/c-ZnO : Al, under illumination there is a photovoltaic effect, while there is none when the contact is not Schottky-like.

Since the same results are obtained when a thin i-ZnO : Al layer is introduced between the semiconductor and the transparent conductive oxide it can be concluded that the contact behaviour is not controlled by the properties of the c-ZnO : Al electrode but by the properties of the γ-In_2Se_3.

5. Conclusion

The dark I–V characteristics of γ-In_2Se_3 based diodes depend on its doping state. Without doping they behave like a Schottky contact while they fit with space charge limited current theory

with traps with distributed energy in the band gap when γ-In_2Se_3 is Mn doped. The same results are obtained when a thin non-conductive i-ZnO : Al buffer layer is introduced between the semiconductor and the conductive c-ZnO : Al electrode. This means that the interface characteristics are controlled by the γ-In_2Se_3 properties. A photovoltaic effect is only present in the case of the Schottky contact. However, the γ-In_2Se_3 resistivity being very high, the effect is small. In the case of γ-In_2Se_3 : Mn its conductivity is far higher but the disordered orientation of the crystallites and the localized states present in the band gap after doping prohibit Schottky contact formation and photovoltaic effect occurrence.

References

[1] Yilmaz K, Parlak M and Ercelebi C 2004 *J. Mater. Sci.: Mater. Electronics* **10** 225
[2] El Maliki H, Marsillac S, Bernède J C, Faulques E and Wery J 2001 *J. Phys.: Condens. Matter* **13** 1839
[3] Vaidyanathan R, Stickney J L, Cox S M, Compton S P and Happek U 2003 *J. Electroanal. Chem.* **599** 55
[4] Amory C, Bernède J C, Halgand E and Marsillac S 2003 *Thin Solid Films* **431–432** 22
[5] Likforman A, Carré D and Hillel R 1978 *Acta. Cryst.* B **34** 1
[6] Pfitzner A and Lutz H D 1996 *J. Solid State Chem.* **124** 305
[7] Amory C, Bernède J C and Marsillac S 2003 *J. Appl. Phys.* **94** 6945
[8] Amory C, Guettari N, Bernède J C and Mebarki M 2006 *Phys. Status Solidi* a **203** 3726
[9] Assmann L, Bernède J C, Drici A, Amory C, Halgand E and Morsli M 2005 *Appl. Surf. Sci.* **246** 159
[10] Yamaguchi T, Tanaka T and Yoshida A 2002 *J. Vac. Sci. Technol.* A **20** 1755
[11] Scofield J H, Duda A, Ablin D, Ballard B L and Predecki P K 1995 *Thin Solid Films* **260** 26
[12] Bichel R and Levy F 1985 *Thin Solid Films* **124** 75
[13] Joint Committee on Powder Diffraction Standards, JCPDS 40-1407
[14] de Groot C and Moodera J S 2001 *J. Appl. Phys.* **89** 4336
[15] Jasinki J, Swider W, Washburn J, Liliental-Weber Z, Chaïken A, Nauka K, Gibson G A and Yang C C 2002 *Appl. Phys. Lett.* **81** 4356
[16] Joint Committee on Powder Diffraction Standards, JCPDS 86-1397
[17] Burstein E 1954 *Phys. Rev.* **93** 632
[18] Gourmelon E, Lignier O, Hadouda H, Couturier G, Bernède J C, Tedd J, Pouzet J and Salardenne J 1997 *Sol. Energy Mater. Sol. Cells* **46** 115
[19] Tribusch H 1979 *Sol. Energy Mater* **1** 257